

Observation of Physical Parameters in Cu-based SMA Aged Under Constant Pressure

Ş. Nevin BALO, Hawbir Swara Ahmed MANGURI

Department of Physics, Faculty of Science, University of Firat, 23119 Elazig, Turkey

In this study, (wt%) Cu-13.5Al-4Ni shape memory alloy was used. The alloy samples were aged under the constant pressure of 558 MPa at different times. Physical parameters of Cu-13.5Al-4Ni alloy samples aged under constant pressure were examined. The effects on thermodynamic parameters were determined by differential scanning calorimetry (DSC). Microstructural examination was performed by X-ray diffraction (XRD). Metallographic observations were used to verify microstructural changes and microhardness measurements were taken. The physical parameters of the samples aged at different times under constant pressure were compared with the homogeneous sample.

Keywords: Aging, Pressure, CuAlNi shape memory alloy, Microhardnes, Crystallite size.

Submission Date: 29 April 2021

Acceptance Date: 27 July 2021

*Corresponding author: nbalo@firat.edu.tr.

1. Introduction

Shape memory alloys (SMA) have advanced significantly technologically in the previous decade, allowing them to be used as functional materials. The first-order displacive and diffusionless martensitic transformation between a high-temperature austenite phase and a low-temperature martensite phase is related to the functional behavior of these alloys, which is based on shape memory, superelastic, and pseudoelastic phenomena [1-5].

The hardness and strength of some metal alloys can be increased by the uniform distribution of small second phase particles in the matrix phase after appropriate heat treatments. Small phase particles dispersed in the structure are called precipitates. Since the strength of the alloy develops over time, the alloy ages in a sense during this time. For this reason, the process is also called aging hardening or precipitation hardening [6].

Aging is divided into natural and artificial aging. Natural aging takes place over a long period of time and the strength of the material is increased by aging at normal

ambient temperatures. The artificial aging process is done at higher temperatures than room temperature and depending on time. Externally applied stress contributes to artificial aging. The hardening process due to aging accelerates with the increase of the aging temperature and the stress applied [6].

Cu-based SMAs are prone to low-temperature ageing, and a tight control of the post-quench thermal history is required to achieve consistent martensitic transformation behavior. Because these alloys are prone to post-quench aging in high-temperature service circumstances, their transformation temperatures, martensitic phases, and mechanical characteristics can alter over time. To customize the SMA properties, artificial aging can also be used [7,9].

In this study, (wt%) Cu-13.5Al-4Ni shape memory alloy was kept under constant pressure at room temperature for different periods and the effects of pressure on the aging of the alloy were studied.

2. Materials Method

The CuAlNi shape memory alloy used in this study was supplied by Trefimetaux Company, France. The nominal composition is Cu-13.5Al-4Ni (wt%). In order to retain the β phase at room temperature, samples cut from this alloy were annealed in the β -phase-field (1203 K for 30 min.) and later rapidly quenched in iced brine. The aging process of samples was carried out at different times (5 min., 15 min., 30 min., 45 min., 60 min.) 558 Mpa under constant pressure. Differential scanning calorimetry (DSC) measurements were made to determine the transformation temperatures and thermodynamic parameters of homogeneous and aged samples. Perkin Elmer 8000 DSC was used for DSC measurements of samples. DSC measurements were conducted at a scanning heating/cooling rate of 10°C/min. under atmospheric pressure at a temperature range from 30 °C to 200 °C. X-ray diffraction patterns of homogenous and aged samples were taken by Bruker D8 Advance diffractometer in the range of 30°-90°. The X-ray analysis of alloy samples was made by CuK α radiation having a wavelength of 1.54056 Å at room temperature. Following the polishing and chemical etching techniques used on the alloy samples, optical microscope measurements were undertaken. After that, microhardness measurements were taken.

3. Results

3.1. Differential scanning calorimetry measurements

DSC curve of homogenous alloy sample was shown in Fig.1. The transformation temperatures of the alloy samples, A_s , A_f , M_s and M_f were determined using the tangent method. Transformation temperatures of CuAlNi shape memory alloy aged under constant pressure for different times (0, 5 min., 15 min., 30 min., 45 min., and 60 min.) were given in Fig.2. and Table-1 and changes in thermodynamic parameters were given in Table-2. As seen in Fig.1., the alloy sample is in the martensite phase at room temperature. A non-monotonically decrease in transformation temperatures is observed with 558MPa constant pressure applied to homogeneous alloy samples at different times.

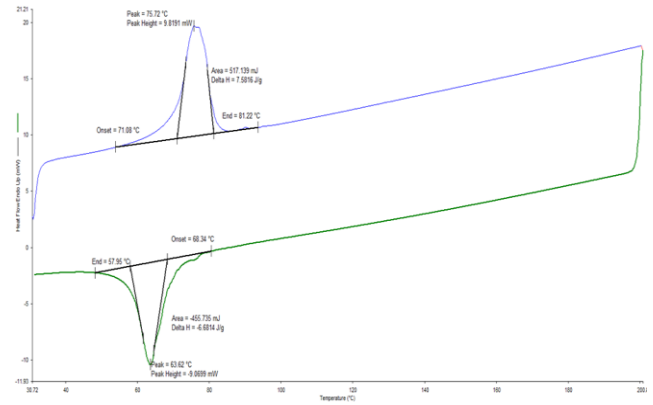


Fig.1. Heating/cooling curve of homogeneous CuAlNi shape memory alloy at 10 °C/min.

Table-1. Changes in transformation temperatures of CuAlNi shape memory alloy kept under constant pressure for different times.

Time (Min)	A_s (K)	A_f (K)	M_s (K)	M_f (K)	$(A_f - M_s)$ (K)
0	344.08	354.22	341.34	330.95	12.88
5	343.94	349.10	339.03	329.61	10.07
15	341.84	350.54	339.14	327.08	11.40
30	337.98	350.34	337.72	328.10	12.62
45	335.76	345.15	335.48	318.83	9.67
60	339.64	348.60	340.10	321.81	8.50

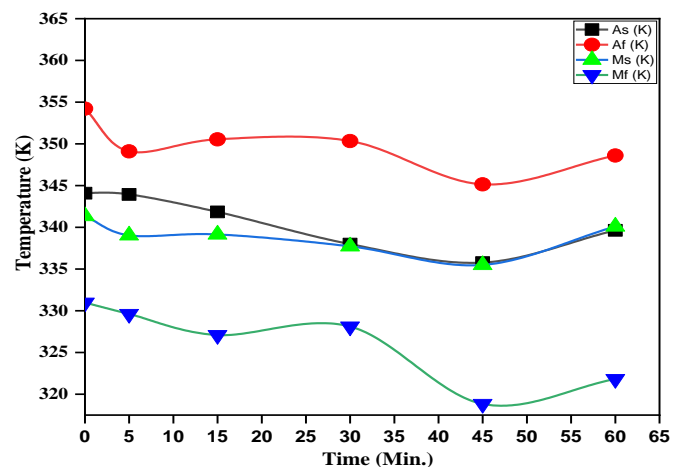


Fig.2. Time-transformation temperatures curve of CuAlNi shape memory alloy aged under 558 MPa constant pressure for different time periods.

Table-2. Changes in thermodynamic parameters of CuAlNi SMA kept under constant pressure for different times.

Time (Min)	T ₀ (K)	ΔH _{M→A} (J/kg)	ΔH _{A→M} (J/kg)	ΔS _{M→A} (J/kg K)	ΔG _{A→M} (J/kg)	G _E (J/kg)
0	347.78	7581.6	-6681.4	21.79	-140.32	226.39
5	344.06	2817.6	-323.3	8.18	-41.14	77.05
15	344.84	1315.3	-721.8	3.81	-21.71	45.94
30	344.03	1079.8	-330.4	3.13	-19.75	30.11
45	340.31	1724.4	-948.1	5.06	-24.43	84.24
60	344.35	2139.9	-1327.2	6.21	-26.39	113.58

These changes in the transformation temperatures also affected the thermodynamic parameters (Table-2). T₀ is the equilibrium temperature and is defined as the critical temperature at which the Gibbs free energies of the austenite and martensite phases are equal. It is calculated with the following expression [10-12].

$$T_0 = (A_f + M_s)/2 \quad (1)$$

The equilibrium temperature of the homogeneous sample is 347.78 K. The equilibrium temperature of the alloy samples aged for different times at 558MPa constant pressure decreased. The mean equilibrium temperature is 344.22 K and its standard deviation is ± 2.384294. The area under the endothermic and exothermic peaks in the DSC curves gives the enthalpy values, ΔH^{M→A} and ΔH^{A→M}. The enthalpy changes of the alloy aged at different times under constant pressure are shown in Fig.3. Entropy is calculated with the following expression [13,14].

$$\Delta S_{M \rightarrow A} = \Delta H_{M \rightarrow A} / T_0 \quad (2)$$

Entropy is a measure of disorder and, as seen in Table-2, and Fig.4. the entropies of alloy samples aged for different times under constant pressure of 558 MPa decreased. With this decrease in entropy, elastic energy also decreased.

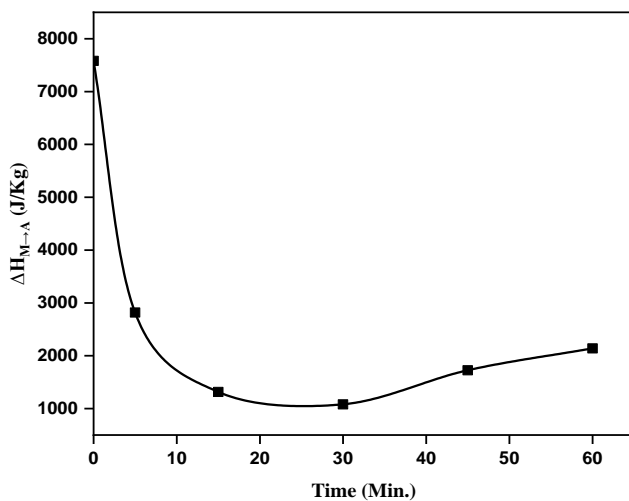


Fig.3. Enthalpy change of CuAlNi shape memory alloy aged under constant pressure of 558Mpa.

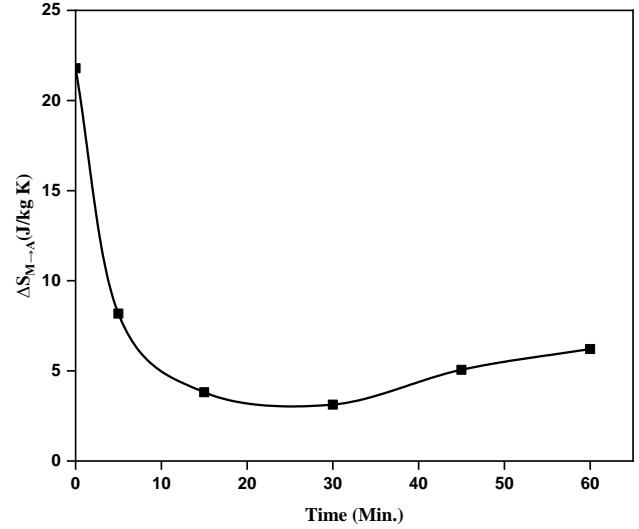


Fig.4. Entropy change of CuAlNi shape memory alloy aged under constant pressure of 558Mpa.

The supercooling T₀-M_s represents the hysteresis in the transformation, which is characterized by the driving force for the nucleation of martensite, ΔG^{A→M} as [13,15],

$$\begin{aligned} \Delta G^{A \rightarrow M}(M_s) &= \Delta G^{M \rightarrow A}(T_0) - \Delta G^{M \rightarrow A}(M_s) \\ &= -(T_0 - M_s)\Delta S^{M \rightarrow A} \end{aligned} \quad (3)$$

ΔG Gibbs free energy changes of the alloy aged at different times under constant pressure are shown in Fig.5.

The elastic energy G_E stored in the self-accommodated martensitic variations is related to the difference M_f-M_s by [14,15]

$$\begin{aligned} \Delta G_E &= \Delta G^{A \rightarrow M}(M_s) - \Delta G^{A \rightarrow M}(M_f) \\ &= (M_s - M_f)\Delta S^{M \rightarrow A} \end{aligned} \quad (4)$$

As seen in Table-2 and Fig.6., the elastic energy of CuAlNi alloy aged under constant pressure was decreased.

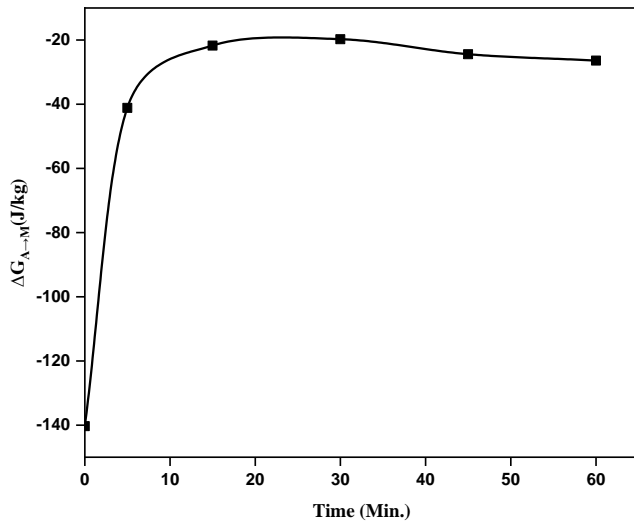


Fig.5. Gibbs free energy change of CuAlNi shape memory alloy aged under constant pressure of 558Mpa.

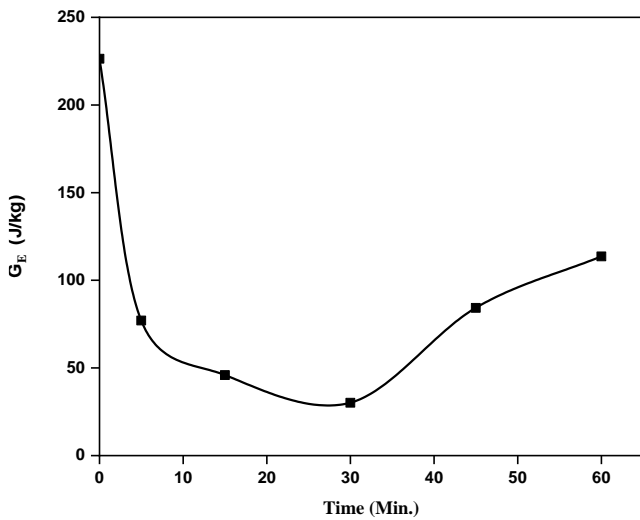


Fig.6. Elastic energy change of CuAlNi shape memory alloy aged under constant pressure of 558Mpa.

3.2. X-ray diffraction (XRD) analysis results

X-ray patterns were used to analyze the structures of CuAlNi shape memory alloy aged under constant pressure for different times. The X-ray patterns of the alloy samples are given in Fig.7. As for the phase shown in Fig.7., one should remind that β_1' martensite has an ordered AlCu_3 type, the γ_1' martensite an ordered Cu_3Ti type structures. Shape memory effect (SME) alloys particularly those of the CuAlNi system may undergo either a single transformation ($\beta_1 \leftrightarrow \beta_1'$ or $\beta_1 \leftrightarrow \gamma_1'$) or a combined transformation ($\beta_1 \leftrightarrow \beta_1' + \gamma_1'$) depending on the composition [16]. As seen in Fig.7. (a), homogeneous CuAlNi shape memory alloy exhibits peaks belonging to β_1' , γ_1' martensite and γ_2 precipitate phase. When the cooling rate of the alloy

is slow, a large number of coarse blocks and dendritic γ_2 phases can easily precipitate in grains or grain boundaries [17]. XRD patterns of alloy samples aged at different times under constant pressure show changes in peak intensities. XRD peaks are compatible with references [18-20]. The crystallite size for the alloy samples were calculated using the Debye Scherrer equation [21,22].

$$D = \frac{0.9\lambda}{FWHM \cos\theta}, \quad (5)$$

where D is crystallite size, λ is the X-ray wavelength, FWHM is the full width at half the maximum peak and θ is the Bragg angle. Crystallite sizes for the alloy samples are given in Table-3. As seen, the crystallite size of CuAlNi alloy aged under constant pressure was decreased.

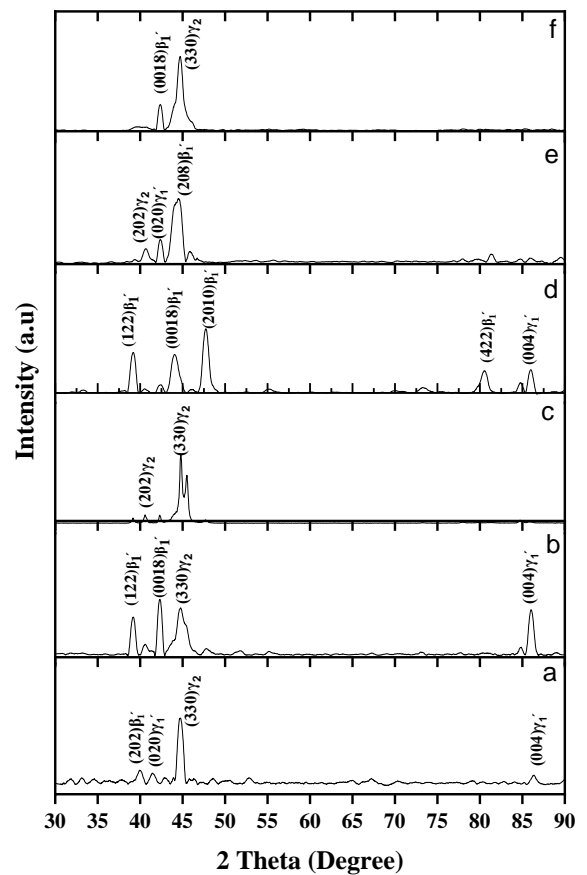


Fig.7. The X-ray diffraction patterns were obtained for different times at constant pressure 558 MPa. a) Homogenous b) 5 min. c) 15 min. d) 30 min. e) 45min. f) 60 min.

3.3. Metallographic observations and microhardness results

Optical images of the CuAlNi shape memory alloy samples are given in Figures 8 (a-f). As can be seen from the images, homogenous CuAlNi shape memory alloy shows martensite structure and precipitate phase at room temperature (Fig.8.-a). Precipitates, different martensite plates (needle-shaped, zigzag and V-shaped martensites), and cracks are seen in the optical photographs of the samples aged for different times under constant pressure at room temperature (Fig.8. b-f) [5,16,23-25].

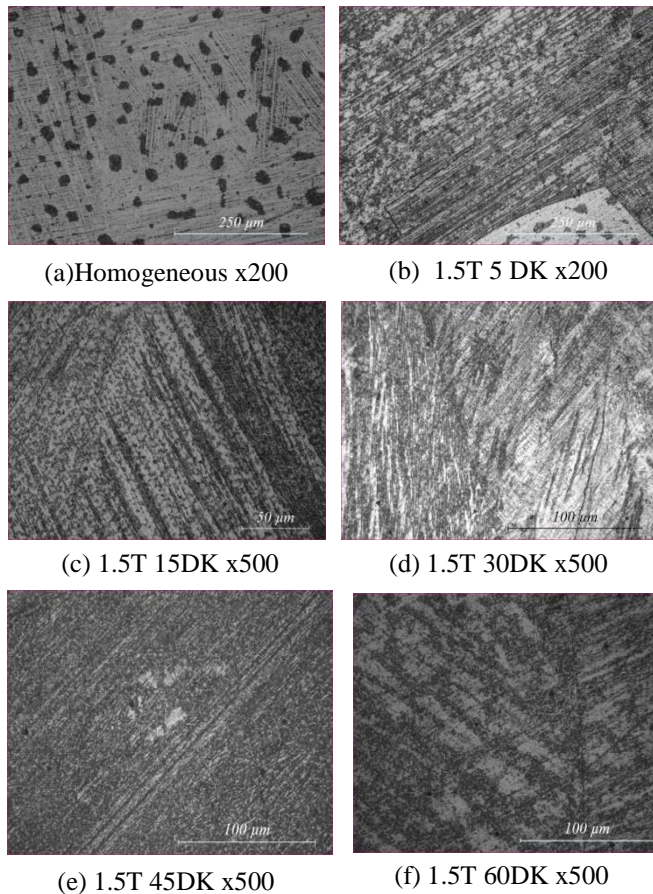


Fig.8. Optical images of CuAlNi SMA after aged under the constant pressure of 558MPa for different times a) 0 X200 b) 5 min. X200 c) 15 min. X500 d) 30 min. X500 e) 45 min. X500 f) 60 min. X500.

The aged CuAlNi shape memory alloy samples were subjected to a 100-gram force (gf) load to measure their microhardness. The average Vickers microhardness values of these alloy samples are given in Table-3. The hardness of the specimen increased with aging.

Table 3. Average Vickers hardness and crystal size of CuAlNi shape memory alloy aged under 558 MPa constant pressure for different time periods.

Time (min.)	Avg. HV _{0.1} Microhardness	Crystallite Size (nm)
0	241.2	33.0462
5	297.6	33.5405
15	290.6	31.7084
30	289.2	24.4006
45	298.0	22.9758
60	282.8	23.9256

4. Conclusion

The effects of pressure on ageing of CuAlNi SMAs were investigated. The constant pressure applied at room temperature was accelerated the aging of the material. The transformation temperatures and equilibrium temperature of CuAlNi shape memory alloy were decreased with aging under constant pressure. The standard deviation in equilibrium temperature is ± 2.384294 . With aging, entropy, elastic energy, and crystal size decreased, and microhardness values increased. The precipitates formed in the structure caused the alloy to harden. Ageing in the alloys causes the formation of intermetallic precipitate particles and has a dominant influence on the transformation temperatures of the alloys. Optical photographs and XRD measurements also confirm this result. The obtained results indicate that the thermodynamic parameters and microstructure were changed of the alloy aged under constant pressure.

Acknowledgments

The study carried out was supported by Firat University Scientific Research Projects Unit (FÜBAP) under project number FF.21.16

References

- [1] Recarte, V., Pérez-Landazábal, J. I., Rodríguez, P. P., Bocanegra, E. H., Nó, M. L., & San Juan, J. Thermodynamics of thermally induced martensitic transformations in Cu–Al–Ni shape memory alloys. *Acta materialia*, 52(13), (2004) 3941-3948. <https://doi.org/10.1016/j.actamat.2004.05.009>
- [2] Alaneme, K. K., Anaele, J. U., & Okotete, E. A. Martensite aging phenomena in Cu-based alloys: Effects on structural transformation, mechanical and shape memory properties: A Critical Review. *Scientific African*, (2021) e00760. <https://doi.org/10.1016/j.sciaf.2021.e00760>

- [3] Saud, S. N., Hamzah, E., Abubakar, T., Refaei, A., & Hosseinian, R. The Influence of γ -irradiation on the Structure and Properties of the Cu-11.5 wt.% Al-4 wt.% Ni Shape Memory Alloys. In *Advanced Materials Research* 845, (2014). 128-132. Trans Tech Publications Ltd.
<https://doi.org/10.4028/www.scientific.net/AMR.845.128>
- [4] Oliveira, J. P., Zeng, Z., Berveiller, S., Bouscaud, D., Fernandes, F. B., Miranda, R. M., & Zhou, N. Laser welding of Cu-Al-Be shape memory alloys: Microstructure and mechanical properties. *Materials&Design*, 148, (2018) 145-152.
<https://doi.org/10.1016/j.matdes.2018.03.066>
- [5] Dora, T. R. K., Sampath, V., Li, Y., & Hodgson, P. In vitro cytotoxicity and corrosion studies of some copper base shape memory alloys. *Materials Today: Proceedings*, 4(10), (2017) 10672-10681.
<https://doi.org/10.1016/j.matpr.2017.08.013>
- [6] Callister Jr, W. D., & Rethwisch, D. G. (2020). *Callister's materials science and engineering*. John Wiley & Sons.
- [7] Suresh, N., & Ramamurty, U. Effect of aging on mechanical behavior of single crystal Cu-Al-Ni shape memory alloys. *Materials Science and Engineering: A*, 454, (2007) 492-499.
<https://doi.org/10.1016/j.msea.2006.11.069>
- [8] Suresh, N., & Ramamurty, U. The effect of ageing on the damping properties of Cu-Al-Ni shape memory alloys. *Smart materials and structures*, 14(5), (2005) N47-N51.
[doi:10.1088/0964-1726/14/5/N01](https://doi.org/10.1088/0964-1726/14/5/N01)
- [9] Shivaramu, L., Shivasiddaramaiah, A. G., Mallik, U. S., & Prashantha, S. Effect of ageing on damping characteristics of Cu-Al-Be-Mn quaternary shape memory alloys. *Materials Today: Proceedings*, 4(10), (2017) 11314-11317.
<https://doi.org/10.1016/j.matpr.2017.09.056>
- [10] Wayman, C. M., & Tong, H. C. On the equilibrium temperature in thermoelastic martensitic transformations. *Scripta Metallurgica*, 11(5), (1977) 341-343.
[https://doi.org/10.1016/0036-9748\(77\)90263-0](https://doi.org/10.1016/0036-9748(77)90263-0)
- [11] Tong, H. C., & Wayman, C. M. Characteristic temperatures and other properties of thermoelastic martensites. *Acta Metallurgica*, 22(7), (1974) 887-896.
[https://doi.org/10.1016/0001-6160\(74\)90055-8](https://doi.org/10.1016/0001-6160(74)90055-8)
- [12] Huo, Y., & Zu, X. On the three phase mixtures in martensitic transformations of shape memory alloys: thermodynamical modeling and characteristic temperatures. *Continuum Mechanics and Thermodynamics*, 10(3), (1998) 179-188.
<https://doi.org/10.1007/s001610050088>
- [13] Balo, Ş. N., & Sel, N. Effects of thermal aging on transformation temperatures and some physical parameters of Cu-13.5 wt.% Al-4 wt.% Ni shape memory alloy. *Thermochimica acta*, 536, (2012) 1-5.
<https://doi.org/10.1016/j.tca.2012.02.007>
- [14] Romero, R., & Pelegrina, J. L. Change of entropy in the martensitic transformation and its dependence in Cu-based shape memory alloys. *Materials Science and Engineering: A*, 354(1-2), (2003) 243-250.
[https://doi.org/10.1016/S0921-5093\(03\)00013-3](https://doi.org/10.1016/S0921-5093(03)00013-3)
- [15] Zu, X. T., Zhang, C. F., Zhu, S., Huo, Y., Wang, Z. G., & Wang, L. M. Electron irradiation-induced changes of martensitic transformation characteristics in a TiNiCu shape memory alloy. *Materials Letters*, 57(13-14), (2003) 2099-2103.
[https://doi.org/10.1016/S0167-577X\(02\)01145-X](https://doi.org/10.1016/S0167-577X(02)01145-X)
- [16] Pereira, E. C., Matlakhova, L. A., Matlakhov, A. N., de Araújo, C. J., Shigue, C. Y., & Monteiro, S. N., Reversible martensite transformations in thermal cycled polycrystalline Cu-13.7% Al-4.0% Ni alloy. *Journal of Alloys and Compounds*, 688, (2016) 436-446.
<https://doi.org/10.1016/j.jallcom.2016.07.210>
- [17] Wang, Z., Liu, X. F., & Xie, J. X. Effect of γ_2 phase evolution on mechanical properties of continuous columnar-grained Cu-Al-Ni alloy. *Materials Science and Engineering: A*, 532, (2012) 536-542.
<https://doi.org/10.1016/j.msea.2011.11.019>
- [18] Straumal, B. B., Kilmametov, A. R., López, G. A., López-Ferreño, I., Nó, M. L., San Juan, J., ... & Baretzky, B. High-pressure torsion driven phase transformations in Cu-Al-Ni shape memory alloys. *Acta Materialia*, 125, (2017) 274-285.
<https://doi.org/10.1016/j.actamat.2016.12.003>
- [19] G. S. Yang, J. K. Lee, W. Y. Jang, S. J. Jeong, K. Inoue. Effect of aging and microstructure on mechanical rolling CuAlNi shape memory alloy. *Materials Science Forum* 539 (2007) 3326-3331.
<https://doi.org/10.4028/www.scientific.net/MSF.539-543.3326>
- [20] Izadinia, M., & Dehghani, K. Structure and properties of nanostructured Cu-13.2 Al-5.1 Ni shape memory alloy produced by melt spinning. *Transactions of Nonferrous Metals Society of China*, 21(9), (2011) 2037-2043.
[https://doi.org/10.1016/S1003-6326\(11\)60969-2](https://doi.org/10.1016/S1003-6326(11)60969-2)
- [21] Pelosin, V., & Rivière, A. Structural and mechanical spectroscopy study of the β_1' martensite decomposition in Cu-12% Al-3% Ni (wt.%) alloy. *Journal of alloys and compounds*, 268(1-2), (1998)166-172.
[https://doi.org/10.1016/S0925-8388\(97\)00595-1](https://doi.org/10.1016/S0925-8388(97)00595-1)

- [22] Cullity, B. D. (1956). Elements of X-ray Diffraction. Addison-Wesley Publishing.
- [23] Balo, Ş. N., & Yakuphanoglu, F. The effects of Cr on isothermal oxidation behavior of Fe–30Mn–6Si alloy. *Thermochimica Acta*, 560, (2013) 43-46.
<https://doi.org/10.1016/j.tca.2013.03.005>
- [24] Mallik, U. S., & Sampath, V. Effect of composition and ageing on damping characteristics of Cu–Al–Mn shape memory alloys. *Materials Science and Engineering: A*, 478(1-2), (2008) 48-55.
<https://doi.org/10.1016/j.msea.2007.05.073>
- [25] Pereira, E. C., Mathlakova, L. A., da Silva Figueiredo, A. B. H., Lima, E. S., dos Santos Paula, A., & Monteiro, S. N., Grain ejection associated with thermocycling of Cu-Al-Ni shape memory alloy. *Materials Letters*, 210, (2018) 54-57.
<https://doi.org/10.1016/j.matlet.2017.08.123>